Macromolecular Research, Vol. 10, No. 2, pp 60-66 (2002)

Polyetherimide/Dicyanate Semi-interpenetrating Polymer Networks Having a Morphology Spectrum†

Yu-Seung Kim

Department of Chemistry, Virginia Tech., Blacksburg, VA, 24061, USA

Hyun-Sung Min

LG Chemical Ltd. Research Park, 104-1, Moonjidong, Yusongku, Taejon 305-380, Korea

Sung-Chul Kim*

Center for Advanced Functional Polymers, Korea Advanced Institute of Science and Technology, Kusongdong, Yusongku, Taejon 305-701, Korea

Received Dec.18, 2001 ; Revised Feb. 4, 2002

Abstract: The morphology, dynamic mechanical behavior and fracture behavior of polyetherimide (PEI)/dicyanate semi-interpenetrating polymer networks (semi-IPNs) with a morphology spectrum were analyzed. To obtain the morphology spectrum, we dispersed PEI particles in the precured dicyanate resin containing 300 ppm of zinc stearate catalyst. The semi-IPNs exhibited a morphology spectrum, which consisted of nodular spinodal structure, dual-phase morphology, and sea-island type morphology, in the radial direction of each dispersed PEI particle due to the concentration gradient developed by restricted dissolution and diffusion of the PEI particles during the curing process of the dicyanate resin. Analysis of the dynamic mechanical data obtained by the semi-IPNs demonstrated that the transition of the PEI-rich phase was shifted toward higher temperature as well as becoming broader because of the gradient structure. The semi-IPNs with the morphology spectrum showed improved fracture energy of 0.3 kJ/m^2, which was 1.4 times that of the IPNs having sea-island type morphology. It was found that the partially introduced nodular structure played a crucial role in the enhancement of the fracture resistance of the semi-IPNs.

Keywords : dicyanate, toughening, morphology, semi-IPNs, gradient.

Introduction

The toughening of thermoset materials using high performance thermoplastic has recently received attention because the toughened thermosets usually possess good thermal and mechanical properties. Improved fracture resistance in thermoplastic-modified thermosets has usually been obtained by introducing a secondary phase into the thermoset material via reaction induced phase separation, since homogeneous miscible systems have not exhibited a significant increase in fracture resistance.[1] For this purpose, rigid and thermally stable thermoplastics such as polysulfone,[2-4] polyetherimide (PEI),[5-8] and polyethersulfone[6,9] frequently have been used. In these systems, the thermoplastics are initially soluble in the thermoset resin but undergo phase separation during the curing process.

The degree of toughening for those semi-IPNs strongly depends on the morphology, which is mainly influenced by the initial thermoplastic concentration. That is, at a lower thermoplastic concentration (typically below 10%), a sea-island type morphology, in which thermoplastic-rich phases segregate into spherical domains of about 1 μm diameter within the thermoset matrix, provides a moderate increase in fracture toughness. On the other hand, at a higher thermoplastic concentration (typically above 20%), a substantial increase in fracture toughness is obtained due to a co-continuous nodular structure. In the co-continuous nodular structure, spherical nodules of thermoset-rich phase were connected to each other in a continuous thermoplastic matrix. Although the co-continuous nodular structure has the advantage of improvement of fracture toughness, one should be aware of the fact that other properties, like thermal resistance or solvent resistance, are deteriorated by the

†Dedicated to Dr. Un Young Kim on the occasion of his retirement.

*e-mail : kimsc@mail.kaist.ac.kr

generation of a continuous thermoplastic phase.[10,11]

To overcome these drawbacks, we introduced "a morphology spectrum concept" to the thermoplastic modified thermoset materials that has been described in previous papers.[12,13] To obtain the morphology spectrum, we inserted a soluble thermoplastic film into neat thermoset resin, controlled the relative rate of the dissolution and diffusion of the inserted film, and controlled the curing reaction. The fully cured thermoset resin revealed three different types of morphology along the thickness direction because of the thermoplastic concentration gradient formed: co-continuous nodular structure where the concentration of thermoplastic was 20% or more, sea-island type morphology where the concentration of thermoplastic was 10% or less, and dual-phase morphology having both co-continuous nodular structure and sea-island morphology where the thermoplastic concentration was around 15%. The semi-IPNs having a morphology spectrum exhibited improved fracture toughness as well as improved mechanical and thermal properties with a low overall content of thermoplastic. The morphology spectrum system prepared by inserting thermoplastic film, however, has an anisotropic character, which means that the fracture properties for loading in the direction of the thermoplastic film is greater than that for the transverse loading. Therefore, it is necessary to develop a new technical route for the morphology spectrum formation for general application.

The objective of this study was to explore a novel route for the morphology spectrum formation by dispersion of thermoplastic particles and to find the proper reaction conditions. This was attempted by using a zinc stearate catalyst and also by precuring the thermoset resin before adding the thermoplastic particles. For this study, we prepared PEI/dicyanate semi-IPNs by the dispersion of the preformed PEI particles. Also, the dynamic mechanical properties and fracture behaviors of the semi-IPNs were investigated and compared with the control semi-IPNs having uniform morphology.

Experimental

Materials. Bisphenol-A dicyanate (AroCy B-10, Ciba-Geigy) was supplied as a white, high-purity (>99.5 %) crystalline powder (melting point: 79 °C). The cyclotrimerization of the dicyanate resin is shown in Scheme I. A zinc stearate (ZnSt) catalyst was used to control the reaction rate of the dicyanate resin. Polyetherimide (Ultem 1000, General Electric Co., $\overline{M_n}$ = 18,000) (PEI) was used as the thermoplastic component. All materials were used as received from the manufacturer.

Specimen Preparation. The PEI/dicyanate semi-IPNs with a morphology spectrum were prepared by dispersion of PEI particles in precured dicyanate resin. In order to prepare PEI particles, the PEI pellets were first dissolved in chloroform to obtain a 4 wt% solution. The solution was sprayed

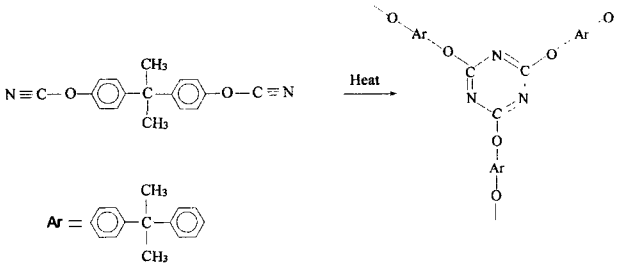

Scheme I. Molecular structure of the dicyanate monomer and the trimerization reaction involved during cure.

in air through a nozzle at room temperature. The residual solvent of the air-dried PEI particles was removed at 150 °C for 4 hr under vacuum. The particles were sieved to obtain relatively uniform particle size. The effective diameter of the particles measured by particle size analyzer (PAMAS system 2120) was 68.8± 13.8 μm. Dicyanate resin with 300 ppm of ZnSt catalyst was precured in an air-convection oven at 180 °C. For this study, four precure conversions (0, 0.25, 0.45, and 0.5) were selected from the dicyanate reaction kinetic data.[10] The prepared PEI particles were added to the precured dicyanate resin and dispersed uniformly by a magnetic spin bar at 180 °C for 30 sec. Subsequently, the mixture was poured into an aluminum mold with dimensions of 70× 70× 2.5 mm, and cured at 180 °C. The total curing time was 6 hr. Post curing was performed in the convection oven at 280 °C for 1.5 hr. The samples were designated as P*X* where *X* represents precure conversion. For example, P0 and P45, represent the precure conversions zero and 45%, respectively. The overall composition of the PEI for this study was 7.5 wt% in the dicyanate resin.

For comparison, a controled sample with uniform concentration was also prepared by conventional solution-mixing techniques.[8] The PEI was dissolved in methylene chloride and mixed with dicyanate resin with 300 ppm of ZnSt catalyst at room temperature. Most of the solvent was evaporated on a hot plate at 40-60 °C and the residual solvent was removed under vacuum conditions at 100 °C for 1.5 hr. The PEI/dicyanate mixture was cured under the same curing conditions.

Measurements. The dynamic mechanical measurement was performed by using a dynamic mechanical thermal analyzer (Rheometrics Scientific DMTA IV) in dual-cantilever bending mode. The dimension of the samples for the test was 35× 10× 2 mm. The measurements were made at a fixed frequency of 1 Hz with a heating rate of 2 °C/min over a temperature range of 50 to 350 °C.

The morphologies of the cured resins were examined using a scanning electron microscope (Philips XL30S). The fractured surfaces of post-cured samples were coated with a thin layer of a gold-palladium alloy. To observe the cross-section of the dried PEI particles before dispersion, the particles were first dispersed in a phenolic resin (resol type),

and the phenolic resin containing the PEI particles was cured in a compression molding machine at 120 °C for 15 min. Next, the cured phenolic resin was polished carefully with a fine abrasive paper until the cross-section of the PEI particles appeared.

The fracture toughness, K_{IC}, was obtained using a single-edge-notch type specimen in a three-point bending geometry as described in ASTM E399-78a. These specimens were cut into rectangular strips with dimensions of 60× 6× 2 mm. A precrack was made by notching the specimen with a diamond wheel and tapping a sharp blade within the notch. Crosshead speed was 1 mm/min. Measured K_{IC} values were converted to critical strain energy release rates, G_{IC}, using the established relationship:

$$G_{IC} = \frac{K_{IC}^2}{E}(1-\nu^2) \quad (1)$$

where Poissons ratio ν was taken as 0.35 for all materials and E is Young's modulus.

Results and Discussion

Morphology of PEI Particles. Figure 1 shows the morphology of the PEI particles prepared by the spray drying process. The PEI particles were somewhat irregular in shape and contained hollow core with diameter of 30-40 μm (see Figure 1(a) and 1(c)). The hollow core was formed due to fast evaporation of the solvent at the surface and hardening of the surface layer during initial stage of the drying process, which restricted the shrinkage of the particles. Besides, the particles had many sub-micron size pores either at the surface or at the inside of the particle (see Figure 1(b) and 1(d)). This porous structure has two effects upon the preparation of the semi-IPNs. First, the porous structure reduces the particle density, which enables the stable dispersion of the PEI particles in the dicyanate resin of relative low density. Second, the porous structure induces the fast diffusion of the dicyanate resin into the PEI particles. Thus, in the particle dispersion system, the dissolution and diffusion time should be shortened compared to the film inserting system and produce a proper concentration gradient for morphology spectrum formation.

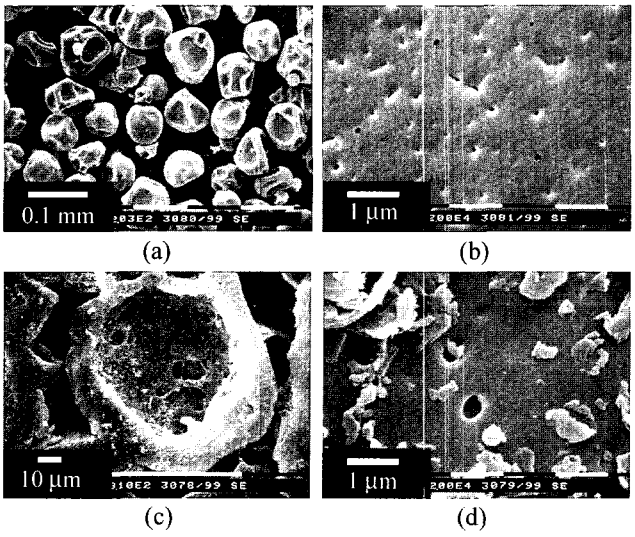

Figure 1. SEM micrographs of the PEI particle surface and cross-section: (a) particle shape; (b) particle surface in high magnification; (c) cross-section of particle in low magnification; (d) cross-section of particle in high magnification.

Morphology of semi-IPNs. The fracture surfaces of the semi-IPNs with various precuring conversions are shown in Figure 2. For the control and P0 semi-IPNs, a sea-island type morphology in which the spherical domains of the PEI-rich phase were uniformly distributed within the dicyanate matrix was observed over all fracture surfaces of the specimen (Figure 2(a)-2(d)). The domain size and the distribution of the PEI-rich phase found in two semi-IPNs were quite similar, which means that the PEI particles completely dissolved and diffused thoroughly into the dicyanate resin before the phase separation and the gelation process occurred.

For the P25 and P45 semi-IPNs, in which the PEI particles were dispersed into precured dicyanate oligomers, macro-sphere domains with a diameter of larger than 90 μm were uniformly distributed in the cross-section of the specimen. Co-continuous nodular structure and dual-phase morphology were found inside the macro-sphere (Figure 2(f) and 2(j)). Both the number and average diameters of the macro-spheres increased as the precure conversion increased from 0.25 to 0.45 (see Figure 2(e) and 2(i)). Table I summarizes the average diameters and volume fractions of the macro-spheres, which were determined directly from SEM micrographs using the known analysis.[12] This result indicated that the P25 semi-IPNs had fewer and smaller regions having a PEI concentration gradient corresponding to the nodular structure or the dual-phase morphology. Based on the previous studies, the nodular structure and the dual-phase morphology were formed when the concentration of PEI was 18 wt% or more and in a range of 12-18 wt%, respectively.[10,13] The size of the dicyanate nodules in the nodular structure gradually increased from the core part of the macro-sphere to the boundary of the dual-phase morphology region because the higher viscosity of the reacting mixture in the core restricted the rate of phase separation (see Figure

Table I. Average Diameter and Volume Fraction of the Macro-scale Domains

Code	Average Diameter (μm)	Volume Fraction
P0	0	0
P25	99.7	0.006
P40	140.9	0.092

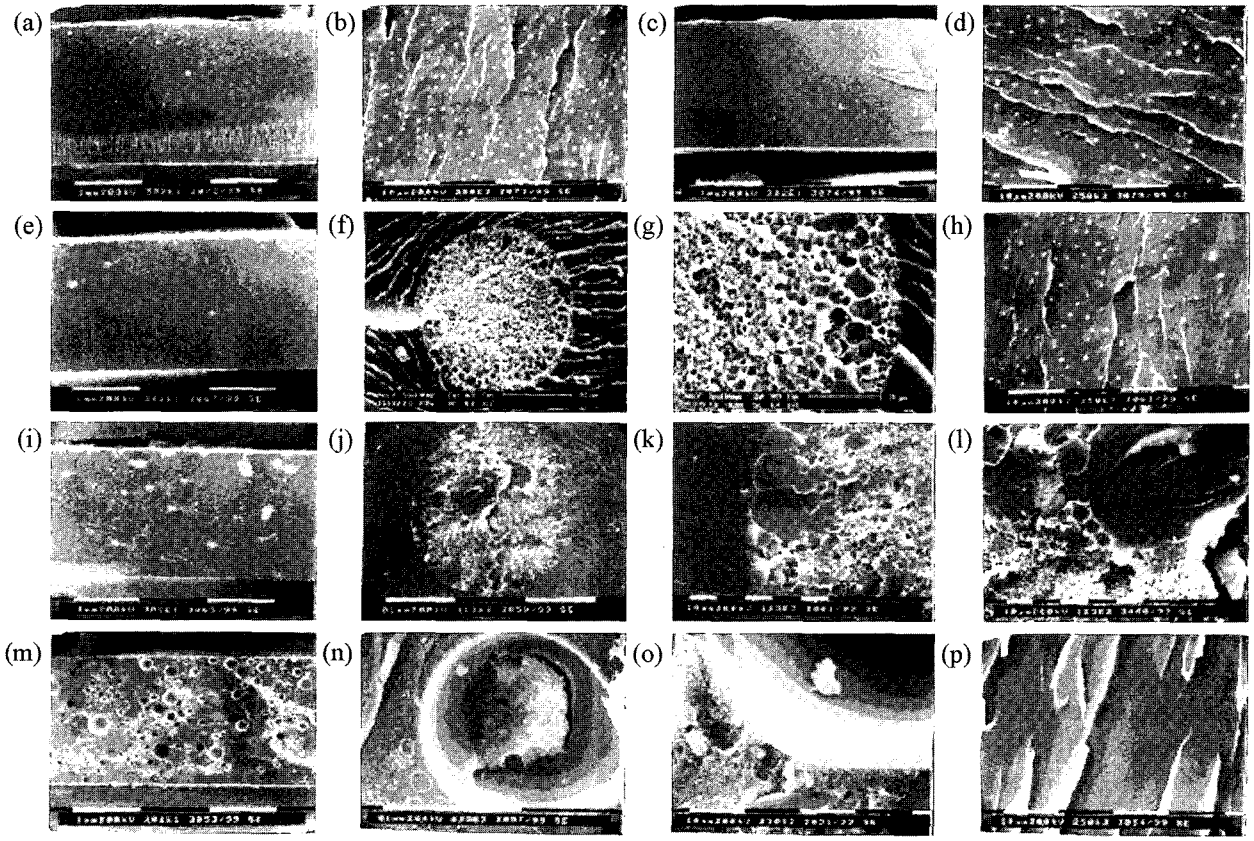

Figure 2. SEM micrographs of semi-IPNs: control = (a) cross-section of whole specimen (b) sea-island morphology region; P0 = (c) cross-section of whole specimen (d) sea-island morphology region; P25 = (e) cross-section of whole specimen (f) macro-scale domain (g) nodular structure region; (h) sea-island morphology region; P45 = (i) cross-section of whole specimen, (j) macro-scale domain, (k) boundary region of the macro-scale domain, (l) dual-phase morphology region; P50 = (m) cross-section of whole specimen, (n) trace of extracted PEI particle, (o) nodular structure region, (p) region without morphology.

2(g) and 2(k)).

Dual-phase morphology through the secondary phase separation, which is sometimes referred to as phase-in-phase morphology,[6,15] was also found inside the macro-scale domain (Figure 2(l)). In the region showing the dual-phase morphology, large dicyanaterich domains with a diameter of about 40 μm were surrounded by the nodular structure containing relatively small dicyanate nodules; inside the large dicyanate-rich domains, small PEI-rich domains with a diameter of about 0.8 μm were found. Most of the dual-phase morphology regions were located near the boundary of the macro-sphere, but occasionally they were found in the core part of the macro-sphere because of the relative low concentration of PEI due to the hollow core of the preformed PEI particles (see Figure 2(j)).

Outside of the macro-sphere, sea-island type morphology was observed (Figure 2(h)). That is, many micro-spherical PEI-rich phases were located at a distance from the boundary of the macro-sphere.

For the P50 semi-IPNs, both voids and traces of the extracted PEI particles were observed in the fractured specimens (Figure 2(m) and 2(n)). The voids might be formed due to the high viscosity of precured dicyanate resin during mixing or the curing step. Outside the extracted PEI particles, a nodular structure containing very small dicyanate nodules (less than 0.5 μm diameter) was observed (Figure 2(o)). Outside of the nodular structure region, however, no sea-island type morphology was found, presumably because the gelation of dicyanate resin occurred in a very short time before the nucleation and growth mode of phase separation occurred (Figure 2(p)).

Dynamic Mechanical Properties. It has been known that the dynamic mechanical behaviors of thermoplastic/thermoset semi-IPNs were strongly dependent upon the phase composition and the morphology.[7,16,17] In particular, the T_g change of the phase-separated domains in each composition of semi-IPNs exhibited interesting features. Figure 3 shows the influence of PEI contents on the loss modulus, E'', of the PEI/dicyanate semi-IPNs with uniform morphology. The semi-IPNs had two separate glass transition temperatures.

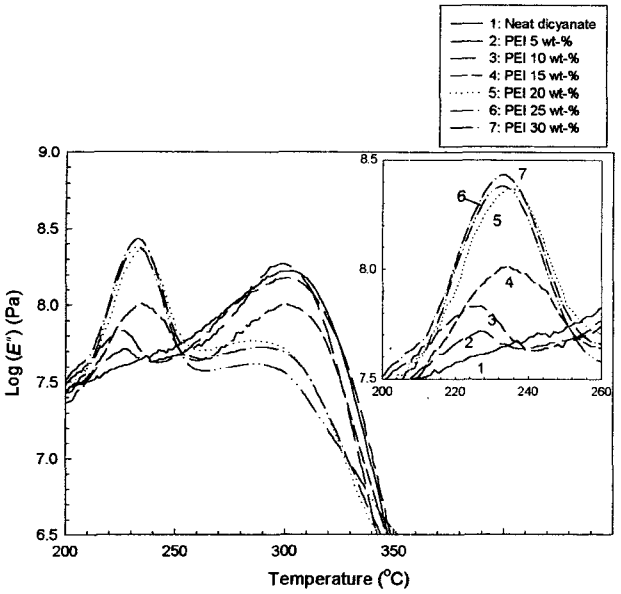

Figure 3. Loss modulus (E'') change with temperature of the PEI/dicyanate semi-IPNs with uniform morphology.

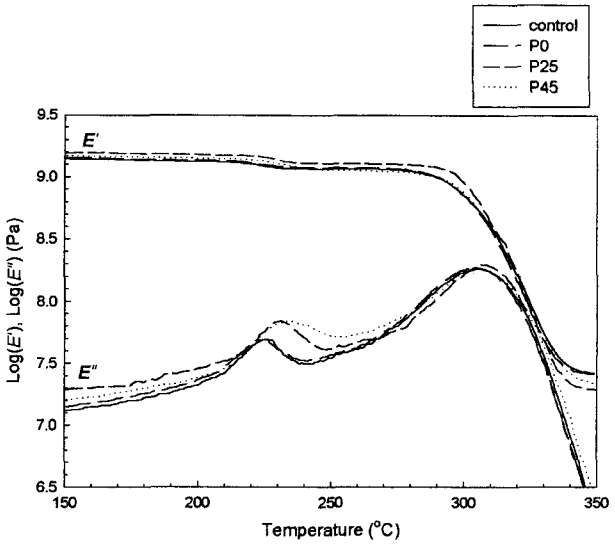

Figure 4. Dynamic mechanical behaviors of the semi-IPNs prepared by dispersion of PEI particles.

The lower temperature relaxation near 230 °C corresponds to the glass transition of the PEI-rich phase, while the higher temperature relaxation near 300 °C is associated with the glass transition of the dicyanate-rich phase. The results indicated that as the thermoplastic concentration increased, the peak height of E'' for the PEI-rich phase gradually increased while the peak height of E'' for the dicyanate-rich phase decreased. The T_g change of the PEI-rich phase, on the other hand, shows a discontinuity at 15 wt% PEI (see the magnified plot in Figure 3). That is to say, the T_g of the PEI-rich phase increased and reached a maximum at around 15% thermoplastic concentration, in which the sea-island type morphology changed to a dual-phase morphology. These features can be explained: the compositional differences of each phase produced via a spinodal decomposition mode of phase separation, which occurs in the 15-60% thermoplastic compositional range, are smaller than the compositional differences produced via a nucleation and growth mode of phase separation.

Figure 4 shows the temperature dependence of the storage modulus, E', and loss modulus, E'', of the semi-IPNs prepared by the particle dispersion method. The P25 and P45 semi-IPNs, in which had a morphology spectrum, showed transition temperature shifts of the PEI-rich phase toward high temperature. Considering the T_g change of the PEI-rich phase found in semi-IPNs with uniform morphology, these transition temperature shifts are due to the partially formed co-continuous nodular structure and the dual-phase morphology, which were predominantly formed via a spinodal decomposition mode of phase separation. The transitions near the T_g of the dicyanate-rich phase, however, were very similar to those of the control sample of uniform morphology, as depicted in Table II. This is due to the structure that the continuous dicyanate matrix contains the isolated macro-sphere domains.

Table II. Transition Temperature of Each Phase Determined by Loss Modulus

Sample Code	Transition Temperature	
	PEI-rich Phase	Dicyanate-rich Phase
Control	223	306
P0	224	305
P25	231	306
P45	235	307

Other features of the dynamic mechanical behavior of the morphology spectrum system were characterized by broad transitions of the PEI-rich phase. These broad transitions would be related to the magnitude of the concentration gradient due to the continuous change of the concentration in the phase-separated state. Similar effects related to the broad range of transition temperatures were found in gradient copolymers.[18]

On the other hand, the P0 semi-IPNs, which had only sea-island morphology, shows very similar dynamic mechanical behaviors to the control semi-IPNs, which indicated that the morphology and composition of both these semi-IPNs are similar.

Fracture Toughness. Fracture resistance of the cured semi-IPNs showed a significant dependence on morphology. Figure 5 shows the critical strain energy release rates, G_{IC}, for the cured semi-IPNs. The P45 semi-IPNs, which had a large number of macro-spheres, showed the highest

fracture resistance of 0.37 kJ/m^2, about 1.4 times higher than the control or P0 semi-IPNs having uniform sea-island type morphology. The large increase in fracture toughness produced by the morphology spectrum is probably related to the different toughening mechanism. Figure 6 shows the fracture surface of each morphology region after fracture test.

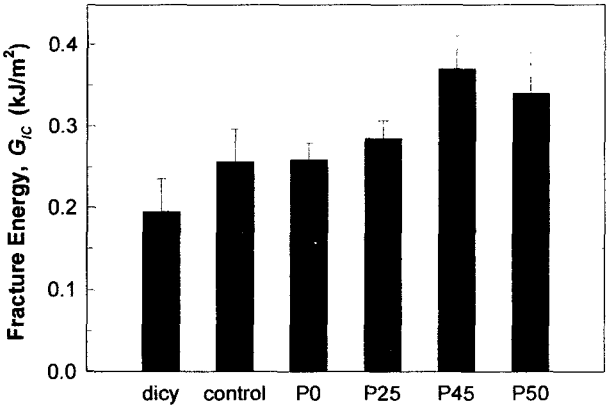

Figure 5. Fracture energy, G_{IC}, of the semi-IPNs prepared by dispersion of PEI particles; The dicy denotes the unmodified dicyanate resin.

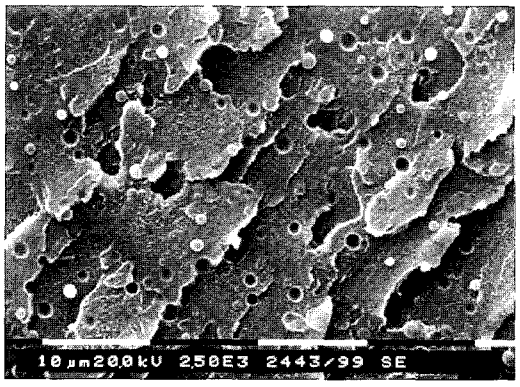

(a)

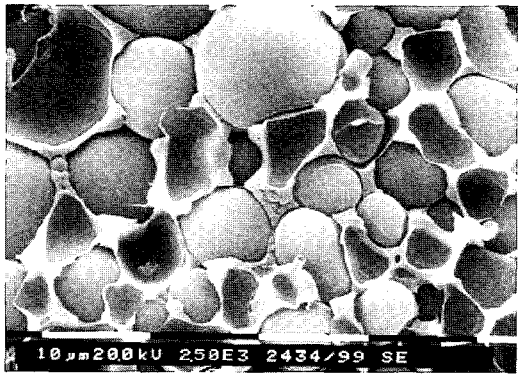

(b)

Figure 6. Fracture surface of each morphology region found in P45 semi-IPNs (a) sea-island morphology region; (b) nodular structure region.

Figure 6(a) shows that the major toughening of sea-island type morphology was obtained through crack deflection and crack pinning by the isolated PEI-rich domains, while the nodular structure region showed extensive deformation of the PEI continuous phase, which presumably contributed significantly to the fracture energy (Figure 6(b)). That is to say, the control or P0 semi-IPNs, which had sea-island morphology only, were toughened only through crack deflection or crack pinning toughening mechanism, while P45 semi-IPNs, which had nodular structure and dual-phase morphology as well as sea-island morphology, absorbed fracture energy mainly by the plastic deformation of the continuous PEI-rich phase.

Analysis of SEM micrographs suggested another toughening effect induced by the macro-sphere morphology region. Figure 2(f) shows that a tail-like crack bifurcation parallel with the crack growth direction was formed behind the macro-sphere. The tail-like structure was formed because the bifurcated crack continued on different planes, when the crack progresses around the heterogeneous region, thereby providing greater crack growth resistance.[19] Thus, this tail formation could partially contribute to the improved fracture resistance by creating new fracture surfaces.

The P50 semi-IPNs showed an improved G_{IC} value compared to the control semi-IPNs, in spite of the fact that the specimen contained many voids and a few nodular structures. This is presumably because dewetting of the PEI particles occurs during the fracture test. It is known that the new surface generation during the fracture test contributes to an increase in the fracture resistance.[20]

Figure 7 shows the correlation between the G_{IC} and the volume fraction of the nodular and dual-phase morphology. The unfilled squares represent the morphology spectrum

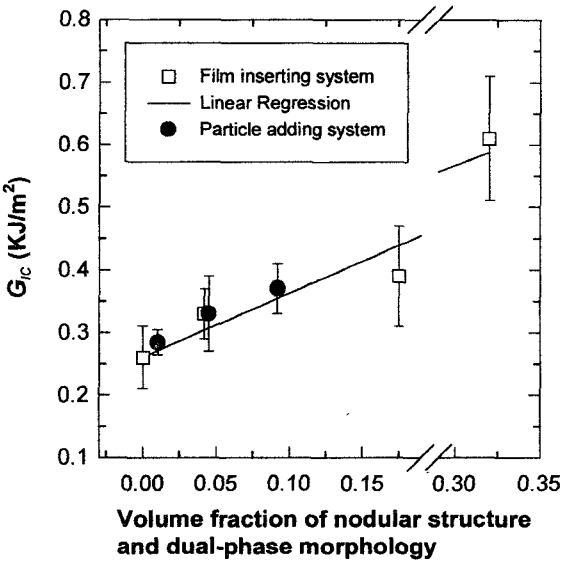

Figure 7. Fracture energy change with the volume fraction of nodular structure and dual-phase morphology.

system prepared by inserting PEI film,[13] and the filled circles belong to the semi-IPNs prepared by dispersion of PEI particles. Figure 7 indicates that there is a linear correlation of the fracture energy with the volume fraction of the nodular structure and dual-phase morphology within error bounds. These results support the hypothesis that the toughening effect of the morphology spectrum system is principally obtained by plastic deformation of the continuous PEI-rich phase in the nodular structure and dual-phase morphology.

Conclusions

Another preparation route for the formation of a morphology spectrum in PEI/dicyanate semi-IPNs was explored. PEI particles were prepared by a spray drying process. SEM micrographs showed the prepared particles with an average diameter of 69 μm contained both a macrovoid and submicron size pores inside the particles. The control of the concentration gradient for the morphology spectrum formation was performed by precuring the dicyanate before mixing with the PEI particles. The semi-IPNs without precuring did not exhibit the morphology spectrum, while at precure conversions of 0.25 and 0.45, spherical macro-scale domains appeared. In the macro-scale domains, nodular structure and dual-phase morphology were developed in the radial direction with the PEI concentration. When the precure conversion was 0.5, some voids and traces of extracted PEI particles were observed. A partially nodular structure composed of very small dicyanate nodules was formed near the extracted PEI particles.

Dynamic mechanical data of the semi-IPNs with a morphology spectrum indicated the following features; 1) the transition of the PEI-rich phase was shifted toward higher temperatures because the nodular structure via spinodal decomposition was introduced; 2) the transition of the PEI-rich phase was broader than that of the control because the semi-IPNs had a concentration gradient in the phase-separated state.

The semi-IPNs prepared by adding PEI particles showed improved fracture toughness. For example, the fracture energy of P45 was 0.37 kJ/m^2, which was 1.4 times that of the control semi-IPNs showing only sea-island morphology. The fracture energy was linearly proportional to the volume fraction of the nodular structure and dual-phase morphology within error bounds.

Acknowledgments. This study was supported by the Center for Advanced Functional Polymers, which was funded by the Korea Science & Engineering Foundation (KOSEF), Taejon, Korea.

References

(1) M. C. Chen, D. J. Hourston, and W. B. Sun, *Eur. Polym. J.*, **28**, 1471 (1992).
(2) A. J. MacKinnon, S. D. Jenkins, P. T. McGrail, and R. A. Pethrick, *Macromolecules*, **25**, 3492 (1992).
(3) B. G. Min, J. H. Hodgkin, and Z. H. Stachurski, *J. Appl. Polym. Sci.*, **50**, 1065 (1993).
(4) P. A. Oyanguren, M. J. Galante, K. Andromaque, P. M. Frontini, and R. J. J. Williams, *Polymer*, **40**, 5249 (1999).
(5) C. B. Bucknall and A. H. Gilbert, *Polymer*, **30**, 213 (1989).
(6) E. M. Woo, D. A. Shimp, and J. C. Seferis, *Polymer*, **35**, 1658 (1994).
(7) B. K. Lee and S. C. Kim, *Polym. Adv. Technol.*, **6**, 402 (1995).
(8) J. W. Park and S. C. Kim, *IPNs around the world*, S. C. Kim and L. H. Sperling, Eds., John Wiley & Sons, Chichester, 1997, Chap. 2.
(9) J. L. Hedrick, I. Yilgor, M. Jurek, J. C. Hedrick, G. L. Wilkes, and J. E. McGrath, *Polymer*, **32**, 2020 (1991).
(10) B. K. Lee, Ph. D thesis, KAIST, Taejon, Korea (1995).
(11) T. H. Yoon, D. B. Priddy, G. D. Lyle, and J. E. McGrath, *Macromol. Symp.*, **98**, 673 (1995).
(12) D. Chen, J. P. Pascault, H. Sautereau, R. A. Ruseckaite, and R. J. J. Williams, *Polym. Int.*, **33**, 253 (1994).
(13) Y. S. Kim and S. C. Kim, *Macromolecules*, **32**, 2334 (1999).
(14) H. S. Min and S. C. Kim, *Polym. Bull.*, **42**, 221 (1999).
(15) J. W. Hwang, K. Cho, C. E. Park, and W. Huh, *J. Appl. Polym. Sci.*, **74**, 33 (1999).
(16) E. M. Woo, C. C. Su, J. F. Kuo, and J. C. Seferis, *Macromolecules*, **27**, 5291 (1994).
(17) Y. S. Kim, H. S. Min, W. J. Choi, and S. C. Kim, *Polym. Eng. Sci.*, **40**, 665 (2000).
(18) K. Matyjaszewski, D. Greszta, and T. Pakula, *ACS Polym. Preprint*, **38**, 707 (1997).
(19) R. E. Robertson and V. E. Mindroiu, *Polym. Eng. Sci.*, **27**, 55 (1987).
(20) S. W. Koh, J. K. Kim, and Y. W. Mai, *Polymer*, **34**, 3446 (1993).